Chronic Thalamic Stimulation with Three-dimensional MR Stereotactic Guidance

Didier Dormont, Philippe Cornu, Bernard Pidoux, Anne-Marie Bonnet, Alessandra Biondi, Catherine Oppenheim, Dominique Hasboun, Philippe Damier, Elisabeth Cuchet, Jacques Philippon, Yves Agid, and Claude Marsault

PURPOSE: To report a method of electrode implantation in the ventralis intermedius nucleus of the thalamus for the treatment of tremor using a 3-D stereotactic MR imaging technique. **METHODS:** Five patients (three men and two women; mean age, 59 years) with medically refractory tremor had intrathalamic implantation of a stimulating electrode. Stereotactic MR imaging was performed on a 1.5-T unit equipped with an MR-compatible Leksell G stereotactic frame fixed to the patient's head. Calculation of the coordinates of the theoretical target was based on the coordinates of the anterior commissure, the posterior commissure, and the midline sagittal plane as determined via stereotactic MR imaging. During the surgical procedure, the best position for the stimulating electrode was determined by electrophysiological and clinical studies. Postoperative MR control studies were done in all cases to verify the position of the electrode. **RESULTS:** Stereotactic MR imaging allowed precise implantation of the stimulating electrode in all patients. Electrode stimulation produced a 90% reduction of the tremor in two patients, an 80% and 70% reduction in one patient each, and a persistent microthalamotomy-like effect in the fifth patient. Examination of the MR control studies showed that mean error in the positioning of the electrodes was 0.77 ± 0.6 mm (mean ± SD) in the x direction and 0.80 ± 1.02 mm in the y direction. **CONCLUSION:** Although our series is relatively small, the precision achieved with stereotactic MR imaging proves that it can be used with confidence for precise functional neurosurgical procedures.

Index terms: Thalamus; Surgery, stereotactic; Magnetic resonance, in treatment planning

AJNR Am J Neuroradiol 18:1093–1107, June 1997

Stereotactic surgery was applied to the treatment of involuntary movement disorders in humans in the early 1950s (1, 2). Ventrolateral thalamotomy has been used extensively to treat tremor associated with Parkinson disease as well as tremor of other origin (3–5). Since 1968, the use of levodopa has limited the indications for thalamotomy in Parkinson disease. More recently, the limitations of levodopa therapy and advances in stereotactic techniques have led to renewed interest in the surgical treatment of tremor (6–8). High-frequency stimulation of the ventralis intermedius (Vim) nucleus of the thalamus is a newly described nondestructive technique for the surgical treatment of tremor (9, 10). This method is based on the implantation of a stimulating electrode inside the Vim nucleus. The electrode is then used to deliver chronic high-frequency stimulation (more than 100 Hz) via a programmable stimulator that is implanted in the subclavicular region. Placement of electrodes for chronic stimulation of deep brain structures was originally done with ventriculographic guidance. This method is still used for this purpose, as reported in recently published series (9–13), as well as for other functional neurosurgical procedures (14–19). This technique, however, is invasive and can

Received May 1, 1996; accepted after revision February 13, 1997.

Financial support for this study was provided by the Comite´ d'Evaluation et de Diffusion de l'Innovation Technologique (CEDIT) Assistance Publique Hôpitaux de Paris.

From the Departments of Neuroradiology (D.D., A.B., C.O., D.H., C.M.), Neurosurgery (P.C., J.P.), Neurophysiology (B.P.), and the Federation of Neurology, INSERM U289 and Centre d'Investigation Clinique (A-M.B., P.D., Y.A.), Salpêtrière Hospital, Paris VI University; and General Electric Medical System Europe, Buc (E.C.); France.

Address reprint requests to Didier Dormont, MD, Department of Neuroradiology, Bâtiment Babinski, Salpêtrière Hospital, 47 Boulevard de L'Hôpital, 75651 Paris, Cedex 13 France.

AJNR 18:1093–1107, Jun 1997 0195-6108/97/1806–1093

cause headache and meningismus, lengthening the hospital stay (8). Moreover, it has been shown that air ventriculography distorts ventricular anatomy, shifting the third ventricle anteriorly (20, 21).

Some authors have proposed the use of targets derived from computed tomography (CT) and/or magnetic resonance (MR) imaging for functional neurosurgery (22–29). Alterman et al (8) have published results of stereotactic ventrolateral thalamotomy comparing CT- and MR-derived targets obtained via a multimodality correlative imaging technique with the final lesion coordinates as determined by ventriculography and microelectrode recording. They concluded that thalamotomies can be safely performed without ventriculography using their multimodality correlative imaging technique (30). This method, however, has not been established for chronic stimulation techniques with implanted electrodes. With thalamotomy, the destroyed area is larger than the area occupied by the tip of a stimulating electrode, suggesting that the precision required for electrode implantation is greater than that needed for thalamotomy. Thus, it is not straightforward that chronic stimulation techniques can be performed by means of MR guidance even if thalamotomies have been performed with the use of CT- and MR-derived targets. In addition, it has been stated by some authors (9–12) that ventriculography is the technique of choice for these implantations, as it permits easier control of the final position of the electrodes.

Preliminary studies with phantoms and anatomic specimens (31, 32) have shown that it is possible to achieve millimetric precision using MR imaging under stereotactic conditions. We thus undertook a prospective study to evaluate the use of three-dimensional MR imaging to guide the implantation of intrathalamic electrodes in patients with medically refractory tremor.

Materials and Methods

Patients

Five patients with medically refractory tremor were selected for stereotactic implantation of an electrode inside the Vim nucleus of the thalamus. The group comprised three men and two women, ranging in age from 45 to 64 years (mean, 59 years). Four patients had parkinsonian tremor and one had idiopathic essential tremor. The diagnostic criteria for Parkinson disease were tremor and akinetic-rigid syndrome of asymmetric onset; improvement of motor disability with levodopa therapy; lack of symptoms or signs suggesting other degenerative syndromes, such as supranuclear palsy; and lack of pyramidal, cerebellar, pseudobulbar signs, or apraxia. The diagnostic criteria for essential tremor were existence of postural tremor of the arms (independently if it worsened with action or if it was associated with neck and/or voice tremor); absence of other neurologic signs; absence of conditions known to exaggerate physiologic tremor; and absence of treatment with tremorigenic drugs. The tremor was exclusively on the left side in three patients and predominated on the left side in the other two. In all patients, electrodes were implanted in the right thalamus, contralateral to the left-sided tremor.

Preoperative examination of the patients included a study of anamnesis, neurologic assessment, neuropsychological tests, video study of the tremor with and without treatment, and polygraphic recording of the tremor. Intensity of the tremor was also evaluated independently by two neurologists (experts in Parkinson disease) before and after the intervention. Part 3 of the Unified Parkinson's Disease Rating Scale (UPDRS) (33) was used for the patients with Parkinson disease, and the Clinical Rating Scale for Tremor (CRST) was used for the patient with essential tremor (34). A single dose of levodopa was administered to the four patients with Parkinson disease 48 to 72 hours after treatment interruption (acute levodopa testing) to confirm that the tremor was medically refractory (35). All patients also had MR imaging to exclude multiple vascular lesions of the white matter and/or the basal ganglia.

All patients gave written informed consent and the protocol was accepted by the ethical committee of our institution.

MR Acquisition

Stereotactic MR imaging was performed on a 1.5-T unit using an MR-compatible Leksell G stereotactic frame (Elekta Instruments, Stockholm, Sweden). Control studies of the homogeneity of the main magnetic field and of the calibration of the gradients were obtained twice a month. Sedation and local anesthesia were used when fixing the stereotactic frame to the patient's head in the operating room. The patient was then transported to the MR unit and stereotactic MR imaging was performed using MR-adapted fiducial markers. The central landmark was established at the level of the center of the frame's coordinate system (ie, $x = 100$, $y = 100$, and $z = 100$). Four stereotactic MR sequences were performed with a field of view of 24 cm and a matrix size of 256×256: 1) 3-mm-thick axial sections with a 1.5-mm gap were obtained with a T1-weighted spin-echo sequence (500/11/1 [repetition time/echo time/excitations]); 2) a gradient-echo coronal scout image was acquired with parameters of 100/6/1 and a 30° flip angle; 3) 124 1.3-mm-thick axial contiguous sections were obtained with a 3-D spoiled gradient-echo (SPGR) (25/5/1, 25° flip angle) sequence; and 4) 124 1.3-mm-thick contiguous sections were obtained with an axial 3-D

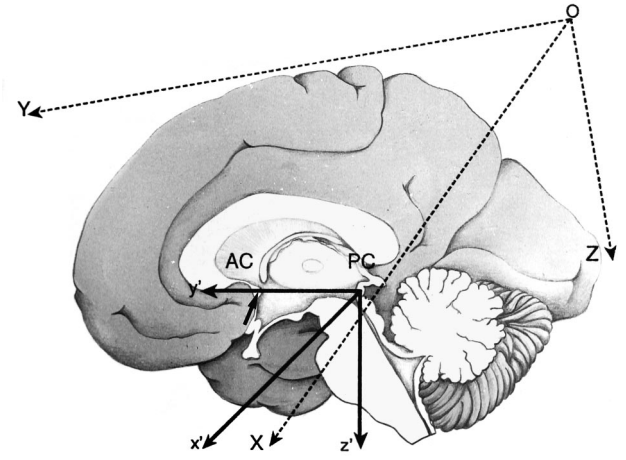

Fig 1. Schematic drawing of the two coordinate systems. The patient's reference system (*P, x', y', z'*) is centered on *PC* with the y' axis passing through *AC* (*arrow*). (*O, X, Y, Z*) is the stereotactic reference system.

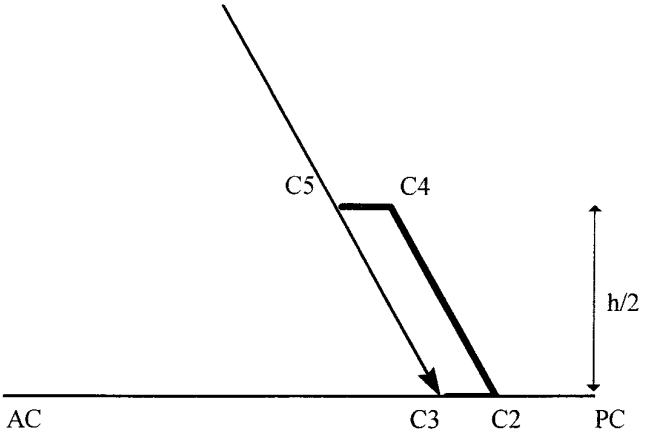

Fig 2. Diagram of the Guiot parallelogram shows the AC-PC plane (the parallelogram is situated at a lateral coordinate of ± (11.5 + V/2), the four corners (C2, C3, C4, and C5) of the parallelogram, and the theoretical trajectory of the electrode in the direction of C3 (*arrow*).

time-of-flight (TOF) angiographic sequence (45/8.7/1, 30° flip angle) after injection of 0.1 mmol/kg gadopentetate dimeglumine. The images were then transferred to an Advantage Windows workstation (General Electric, Buc, France). Measurements of the anteroposterior (120 mm) and the right-left (190 mm) distances between the fiducial markers of the frame on the first axial spin-echo acquisition allowed gradient calibration to be verified. Control of gradient calibration in the z direction was achieved by using the stereotactic software (see below), since it cannot be verified on coronal or sagittal acquisitions, which have significant distortions. If a significant difference (greater than the pixel size) between the apparent distance of the fiducial markers and the real distance had been found, it would have been possible to correct the gradient calibration to perform volumetric acquisitions. However, this was never necessary. After the stereotactic MR procedure, the patients were returned to their room while the electrode trajectories were calculated.

Calculation of the Target and of the Electrode Trajectory: Principle

The Two Coordinate Systems.—For all calculations, we considered two coordinate systems (Fig 1). The first orthogonal coordinate system (P, x', y', z') with the directing vectors (**i', j', k'**) was called the patient's reference system. The center, P, of this reference system was the center of the posterior commissure (PC). The y' axis was defined as passing through the center of the anterior commissure (AC) and, thus, y' was aligned with the AC-PC axis (with y' being positive when directed anteriorly). The (y', P, z') plane was the median sagittal plane, with the z' being positive when directed downward. The x' axis was defined as being perpendicular to the (y', P, z') plane with x' positive when on the left side of the patient. The patient's reference system was thus defined by P (center of PC), by the midline sagittal plane, and by the AC-PC axis. The second coordinate system (O, X, Y, Z) with the directing vectors (**i, j, k**) was the stereotactic coordinate system of the Leksell frame (by definition, the origin, O, of the coordinate system is behind, on the right, and above the patient's head; the x direction being from right to left, y from posterior to anterior, and z from above to below).

Calculation of the Target and Determination of the Theoretical Trajectory in the Patient's Coordinate System.—To calculate the target and trajectory, we used an analytical determination of the Guiot parallelogram (4). This parallelogram (Fig 2) represents the spatial extension of the Vim nucleus in a parasagittal plane. The lower limit of the parallelogram is the AC-PC axis, its upper limit a line parallel to AC-PC and located h/2 mm above it, where h is the height of the thalamus. The posteroinferior (C2) and anteroinferior (C3) corners of the parallelogram are situated 2 × D/12 mm and 3 × D/12 mm, respectively, anterior to the coronal plane (x', P, z'), where D is the length of the AC-PC line, and the posterosuperior (C4) and anterosuperior (C5) corners are 4 × D/12 mm and 5 × D/12 mm, respectively, anterior to the same plane. The distance of the parasagittal plane from the midline was defined as being 11.5 mm + V/2, where V is the width of the third ventricle. This plane is on the right or on the left of the midline, depending on the side of the treated thalamus. In all our procedures, the target chosen was C3, the anteroinferior corner of the Guiot parallelogram, and the theoretical trajectory was chosen parallel to the anterior limit of the parallelogram. This trajectory was entirely defined by the coordinates of the target C3 and of the anterosuperior corner of the parallelogram, C5. Calculations of the coordinates of C3 and C5 in the patients' coordinate systems are straightforward once D, V, and h have been determined (see Appendix).

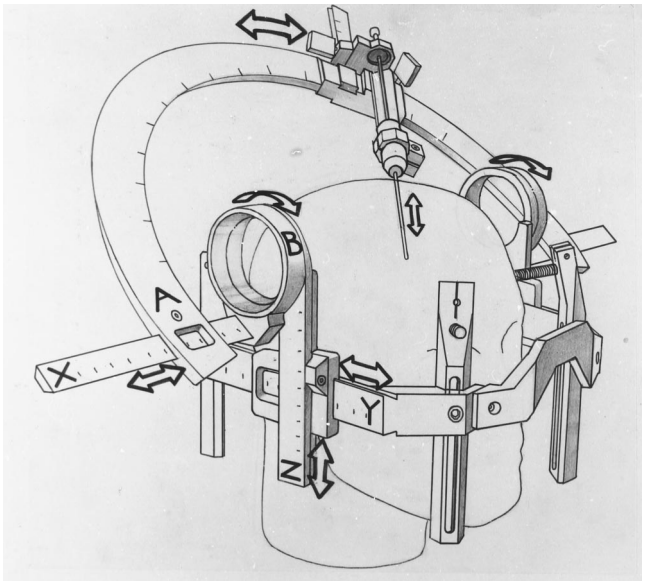

Fig 3. Schematic drawing of the arch of the Leksell stereotactic frame shows the two angles, *A* and *B*.

Calculation of the Target and Determination of the Theoretical Trajectory in the Stereotactic Coordinate System.—Once the patient's coordinates of C3 and C5 are known, they can be obtained in the stereotactic reference system when the transforming coordinate matrix is known. This matrix was calculated with the use of an Excel spreadsheet (Microsoft) on the basis of the stereotactic coordinates of AC, PC, and one point, K, in the middle sagittal plane (see Appendix). The theoretical trajectory was then defined by the target C3 and two angles, denoted A and B, respectively. Angle A is the angle of the trajectory with the rotation axis of the arch (rotation axis of the arch is parallel to the x axis). Angle B is the angle between the (X, O, Y) plane of the frame and the arch of the stereotactic needle-guiding device (Fig 3). A and B are easy to determine in terms of the stereotactic coordinates (x_3, y_3, z_3) of C3 and (x_5, y_5, z_5) of C5.

Calculation of the Target and of the Electrode Trajectory: Application

Determination of the Stereotactic Coordinates of AC, PC, and Point K: Determination of the Width of the Third Ventricle, V, and of the Height of the Thalamus, h—We needed to determine the stereotactic coordinates of AC, PC, and K to calculate the transforming coordinate matrix, M. In addition, we needed to know the width of the third ventricle and the height of the thalamus to calculate the coordinates of C3 and C5. These parameters were obtained on an Advantage Windows workstation, using the Voxtool software (General Electric Europe, Buc, France). The stereotactic SPGR acquisition was transferred to the workstation. The first step consisted of using the Voxtool software to register the volumetric acquisition with the stereotactic reference system. The software can automatically identify all the fiducial markers of the frame once one fiducial marker has been identified manually and can also calculate the mean distance between the theoretical fiducial markers and the actual fiducial markers on the volumetric acquisitions. The value of this mean distance represented a further control of the absence of significant image distortion. The gradient calibration in the z direction was checked using this automatic registration and the value of the mean distance. When the fiducial markers were identified, the acquisition was automatically registered to the stereotactic reference system. The stereotactic coordinates of each point on the acquisition could be obtained by positioning the 3-D cursor on the chosen point. The software also allowed simultaneous visualization of three orthogonal sections and the position of the cursor in these three sections.

After the volume acquisition was registered to the stereotactic reference system, the second step was to determine the midline sagittal plane accurately by using a double oblique section. First, the obliquity of the sagittal section was slightly corrected on an axial section and then corrected again on a coronal frontal view (Fig 4). This procedure allowed us to obtain a section that passed exactly through the midline sagittal plane even if the head of the patient was rotated in relation to the stereotactic frame. The stereotactic coordinates of AC, PC, and point K were then determined in this plane by using the 3-D cursor. The simultaneous visualization of AC and PC on sagittal, frontal, and axial views permitted their precise location (Fig 5). The cursor was positioned on the center of the commissures in all planes. The K point was chosen more than 60 mm from the AC-PC line and approximately in the direction of the trajectory. Interobserver reproducibility of the determined midline sagittal plane and the (P, x', y', z') frame was tested by having two observers independently calculate this plane and the transforming coordinates. The distance between the two midline sagittal planes was then calculated at the level of AC, PC, and a point situated at the same distance from AC, PC, and D/2 mm above the AC-PC plane.

The height of the thalamus was measured as follows (Fig 6): The AC-PC line was located on the midline sagittal plane; a frontal section, perpendicular to the AC-PC line, was determined, equidistant from the AC and PC line; and the distance between the AC-PC line and the upper limit of the thalamus was measured on this frontal section.

The width of the third ventricle was measured at the level of the target; that is, on the AC-PC line, D/4 mm anterior to PC (Fig 7).

Visualization of the Trajectory and Modifications.—Using the stereotactic module of the Voxtool software developed at the Val de Grâce Hospital (Paris, France), we located the trajectory on both the SPGR and the angiographic acquisitions. The trajectory was then slightly modified to avoid the lateral ventricle and vascular structures (Fig 8).

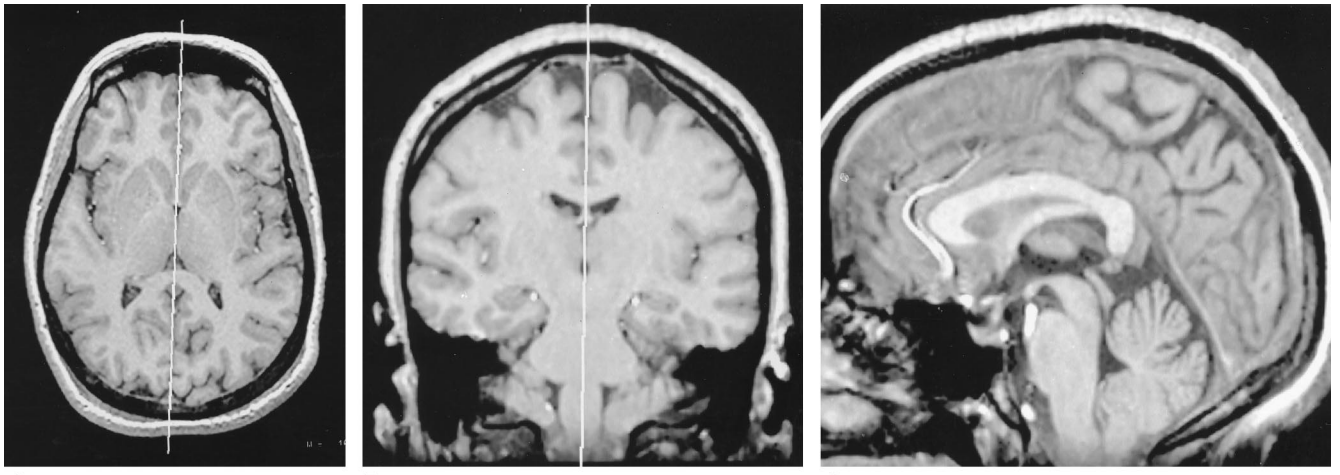

Fig 4. Determination of the midline sagittal plane in case 3.

A, Axial section from the 3-D SPGR MR acquisition (25/5/1, 25° flip angle) shows slight correction of the obliquity of the midline sagittal plane.

B, Second correction of the obliquity of the midline sagittal plane in the coronal plane.

C, Double oblique sagittal reformatted image after the two corrections, situated strictly in the midline sagittal plane.

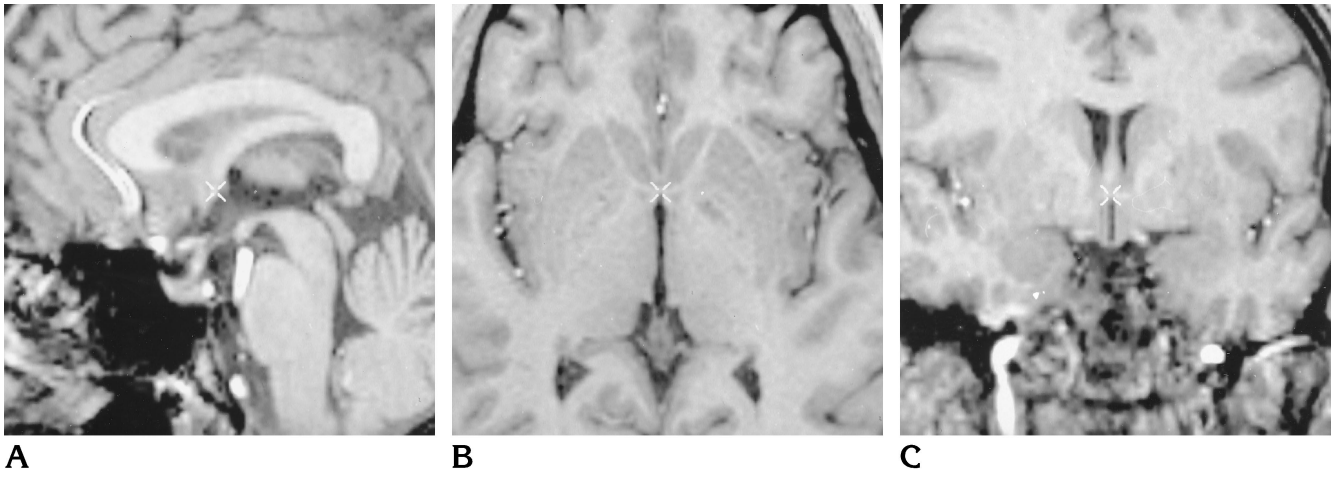

Fig 5. Same patient as in Figure 4. SPGR stereotactic MR (25/5/1, 25° flip angle) determination of the stereotactic coordinates of AC. The center of AC is located precisely by the 3-D cursor, which is seen in the sagittal (*A*), axial (*B*), and coronal (*C*) planes.

Surgical Procedure

For the first patient, the surgical procedure was performed immediately after the trajectory was calculated; in the four other patients, it was done the day after the procedure (stereotactic MR imaging was performed in the evening and the patient slept with the stereotactic frame). In the operating room, the stereotactic needle-guiding device was installed and a burrhole was made, under local anesthesia, at the level of the predetermined trajectory. The direction of the burrhole was also precisely adjusted to fit the trajectory. The first part of the surgical procedure involved the positioning of an exploratory device, consisting of five parallel semi-microelectrodes, to determine the optimal target. The second part involved the implantation of the definitive electrodes.

Neurophysiological and Clinical Studies.—Each surgical electrophysiological study was performed with five FHC (FHC Inc, Brunswick, Maine) semi-microelectrodes moved by means of a step-by-step digital micrometer device. A special electrode holder (Sert, Décines-Lyon) was designed and built to be adapted to the Leksell stereotactic frame (Fig 9). The electrophysiological recording started in the thalamus, 10 mm proximal to the chosen target. The central electrode followed the predetermined trajectory, the other four followed parallel trajectories 2 mm anteriorly, posteriorly, and on each side of the central electrode, respectively. During the step-by-step electrode advancement, cellular units were recorded with the electrodes (impedance of 25 MΩ). At each 1-mm step, an electrical stimulus was delivered alternatively through

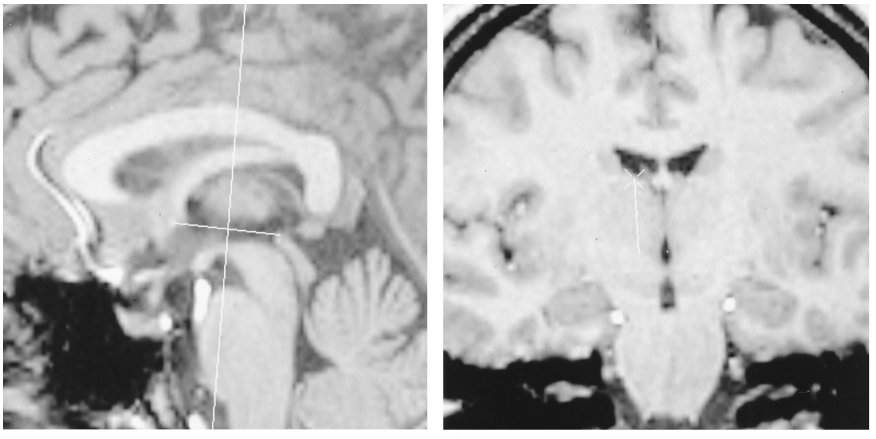

A B

Fig 6. Same patient as in Figures 4 and 5. SPGR stereotactic MR (25/5/1, 25° flip angle) measurement of thalamus height.

A, The AC-PC line is shown; the position of the frontal section is perpendicular to the AC-PC line and equidistant from AC and PC.

B, Thalamus height is measured on the frontal section.

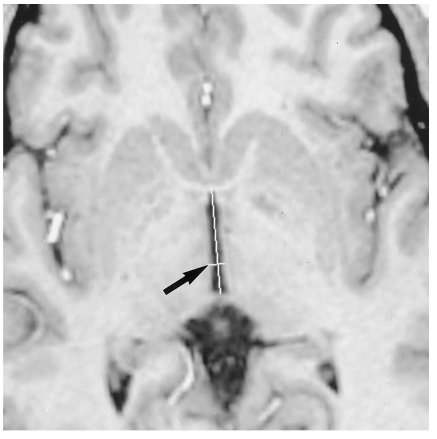

Fig 7. Same patient as in Figures 4 through 6. SPGR stereotactic MR (25/5/1, 25° flip angle) measurement of the width of the third ventricle (*arrow*) at the level of the AC-PC line, D/4 mm anterior to PC.

Fig 8. Same patient as in Figures 4 through 7. Three-dimensional TOF angiographic (45/8.7/1, 30° flip angle) source images. Slight modification of the theoretical trajectory is necessary to avoid the ventricles and/or vascular structures.

A and *B*, Calculated parasagittal trajectory is seen in coronal oblique (*A*) and parasagittal (*B*) planes. The trajectory is extremely near the lateral ventricle.

C and *D*, Chosen trajectory is seen in the coronal oblique (*C*) and parasagittal (*D*) planes. The trajectory now completely avoids the lateral ventricle.

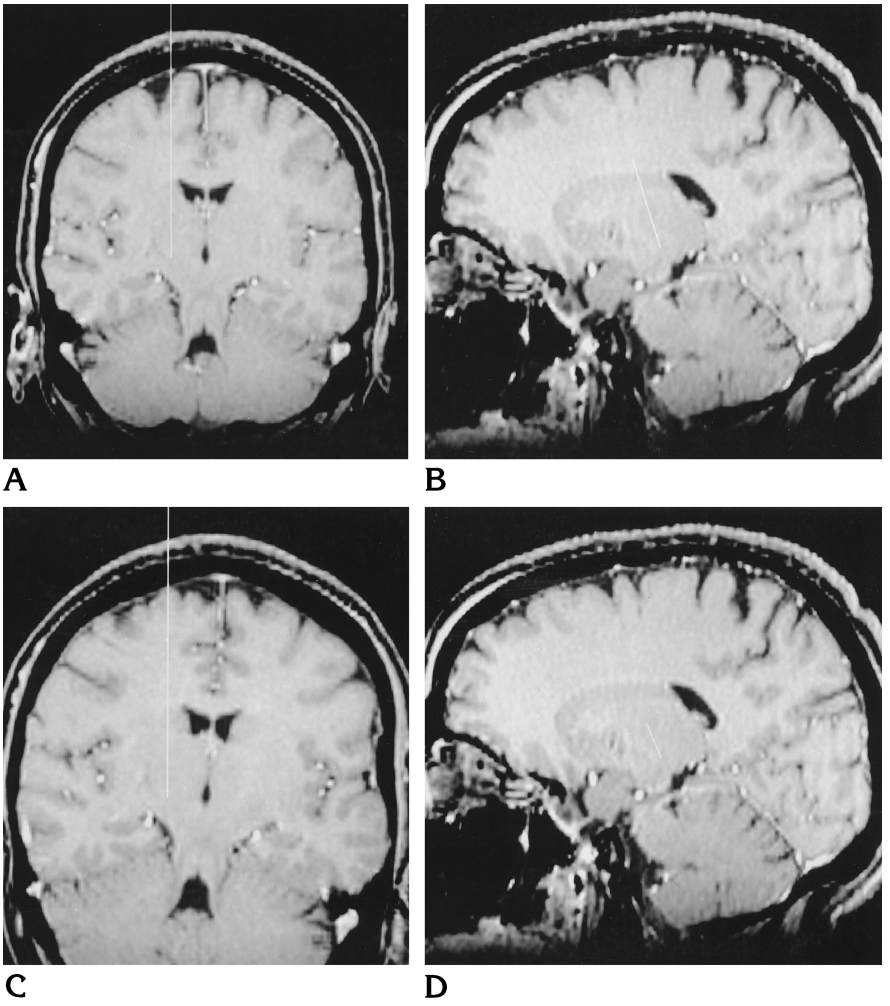

A B

C D

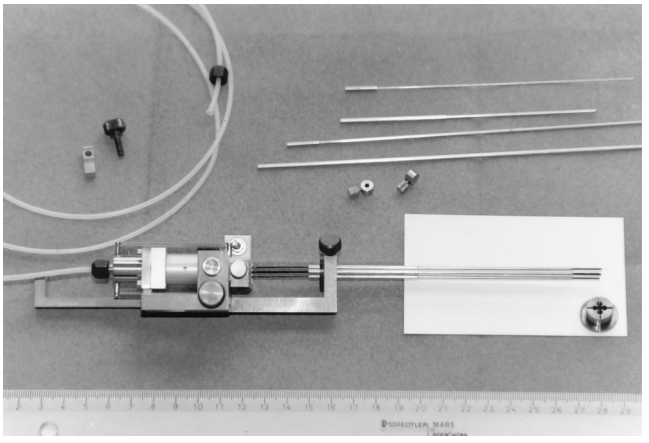

Fig 9. Photograph of the holder of the five exploratory electrodes with the electrodes and a centimeter marker.

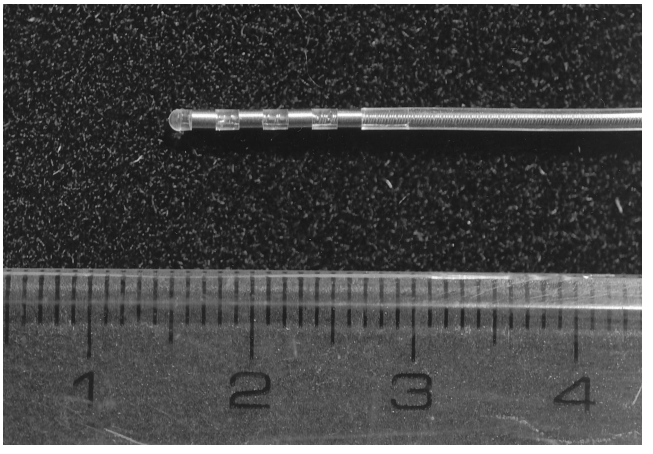

Fig 10. Photograph of the tip of the definitive quadripolar electrode with a centimeter marker.

each of the five semi-microelectrode external tubes (O.7-mm diameter, impedance of 28 KΩ) starting at 0 mA and progressively increasing to a current intensity of 10 mA. Stimuli were negative pulses at 135 Hz (60-microsecond duration). The current was increased until a motor effect (tremor arrest, dystonia), a sensitive effect (paresthesia in the contralateral hand or head territory), or a vegetative effect (nausea) was observed. When tremor arrest was obtained, stimulation was maintained for a few seconds to check whether the effect was transient or persistent. The current intensity threshold allowing the arrest of the tremor was noted for all millimetric steps for each electrode. Current intensity was then increased until the patient reported paresthesia or the 10-mA limit was reached. Current thresholds for paresthesia and tremor arrest were noted. At the end of the electrophysiological study, the current intensity thresholds in relation to the distance (in millimeters) from the electrode to the target were reported on different diagrams using the Excel software. These curves permitted us to choose the best physiological target, defined by the position at which the motor threshold was the lowest and the sensory threshold the highest, for obtaining arrest of the tremor without unpleasant collateral effects.

Neuroradiologic Monitoring.—Radiologic control studies were performed in the operating room to verify that the exploratory electrodes were located at the level of the predetermined trajectory. These studies were obtained by means of the short X-ray device attached to the Leksell stereotactic frame. This device is composed of X-ray–visible fiducial markers and a cassette holder that is fixed to the stereotactic frame itself. The cassette holder keeps the film strictly parallel to the stereotactic frame. With this short X-ray device it was possible to calculate the stereotactic coordinates at the tip of the electrodes during the neurophysiological exploration with two orthogonal views. These coordinates were compared with the calculated trajectory.

Electrode Implantation.—The implanted electrode was an MR-compatible 3387 quadripolar electrode for all patients (Fig 10) (Medtronic, Rueil-Malmaison, France). The optimal exploratory electrode was withdrawn and the definitive electrode was implanted. Radiologic control images were obtained during implantation of the definitive electrode to ensure correct positioning. A quadripolar electrode was used because there is no way to avoid slight postoperative displacement of the contact of an electrode in the direction of its axis. Such displacement can be caused by postoperative displacement of brain tissue or by postoperative fibrosis of the fixation point of the electrode. These modifications could displace the electrode's contact from the target and thus lead to an unsuccessful implantation. The use of a quadripolar electrode avoids this problem in that the stimulating contact can be changed if there is postoperative electrode displacement.

Postoperative MR Control Studies

MR control studies were obtained the day after stereotactic implantation of the electrode in all cases. In these studies, the same SPGR sequence parameters were used as those in the stereotactic MR acquisition. The use of high-field MR imaging to check the position of EEG depth electrodes for seizure monitoring (36) has already been described, and the safety of this procedure has been demonstrated (37). On MR control studies, the coordinates of each contact of the quadripolar electrodes were calculated in the patient's reference system with the same Excel spreadsheet used to calculate the target during the preoperative stereotactic procedure. Coordinates of AC, PC, and one point of the sagittal plane in the MR reference system were introduced, and the Excel spreadsheet then calculated the coordinates of a point in the patient's reference system when its coordinates in the MR reference system were known. The x' and y' coordinates of the electrode at the level of the AC-PC line ($z' = 0$) were calculated from the values of the coordinates of each contact of the electrodes. The x' and y' coordinates were then studied to quantify the precision of the stereotactic MR procedure and to compare the value of the best target from one patient to another. Quantification of the precision of the

TABLE 1: Clinical findings and results in patients with medically refractory tremor treated with chronic electrode stimulation using 3-D MR stereotactic imaging

Case	Sex/Age, y	Type of Tremor	Chosen Trajectory	Thalamotomy-like Effect	Stimulation Voltage	Stimulation Frequency, Hz	Results
1	M/62	Parkinsonian	Anterior	8 mo	NE	NE	Microthalamotomy-like effect
2	M/63	Essential	Posterior	None	1	130	90% tremor diminution
3	F/45	Parkinsonian	Internal	None	2.3	185	90% tremor diminution
4	F/64	Parkinsonian	Central	None	2.8	130	80% tremor diminution
5	M/59	Parkinsonian	Central	None	2.3	185	70% tremor diminution

Note.—NE indicates not evaluable.

stereotactic MR procedure was done by comparing the coordinates of the position of the definitive electrode in the patient's reference system with those used during the procedure. Thus, x' and y' of the target during the procedure were compared with x' and y' of the electrode at $z' = 0$ when the chosen trajectory was the central one. Lateral or anteroposterior corrections were made when the final trajectory was not the central one.

Results

MR Imaging under Stereotactic Conditions

MR imaging under stereotactic conditions was performed in all patients. In each case, the difference between the apparent distance of the fiducial markers and the real distance was less than the size of one pixel, and there was thus no need to correct gradient calibration. The 3-D SPGR stereotactic acquisition gave high-quality images of the brain with good signal/noise and contrast/noise ratios (Figs 4–8). There were no artifacts caused by patients' tremors. In all cases, the exact position of the centers of AC, PC, and the midline sagittal plane was determined and the stereotactic software enabled recognition of the fiducial markers of the frame. Interobserver reproducibility of the determined midline sagittal plane and the (P, x', y', z') frame was excellent: the mean distance between the planes determined independently by the two observers at the level of AC, PC, and the third point (situated at the same distance from AC, PC, and D/2 mm above the AC-PC plane) was 0.27 ± 0.19 mm. The mean distance between the imaged fiducial markers and the model was less than the size of one pixel (0.94 mm) in all patients (0.78 ± 0.14, mean $\pm$ SD). The theoretical trajectories were calculated using the Excel spreadsheet. The MR-angiographic acquisition allowed clear identification of the cortical and subependymal veins. The original theoretical trajectories were adjusted in the five patients to avoid cortical or subependymal veins and to obtain an extraventricular trajectory.

Neurophysiological Studies and Intraoperative Effects of the Stimulation

Electrophysiological exploration allowed recordings of thalamic unitary activities or multiunit cellular discharges. Most cells had a rhythmic firing pattern that was synchronous to the tremor frequency, but others were not. In all patients, the current threshold for tremor arrest, defined by the stimulating current intensity needed to obtain a complete cessation of tremor, decreased as the electrode approached the theoretical target. The position at which the current threshold was minimum (in all cases lower than 0.5 mA) was considered the physiological target.

Among the five electrode trajectories, the best results (ie, those with the lowest threshold for tremor arrest and the highest threshold for unwanted side effects of stimulation) were obtained with the central trajectory in two patients and with the anterior, posterior, and medial trajectories in the other three patients, respectively (Table 1).

Complications

There were no complications related to the procedure. One patient (case 1) had a microthalamotomy-like effect (ie, tremor arrest was obtained during the surgical procedure and it has persisted for 8 months without stimulation by the implanted electrode).

Postoperative MR Results

The 3-D MR images allowed an exact determination of the position of the stimulation elec-

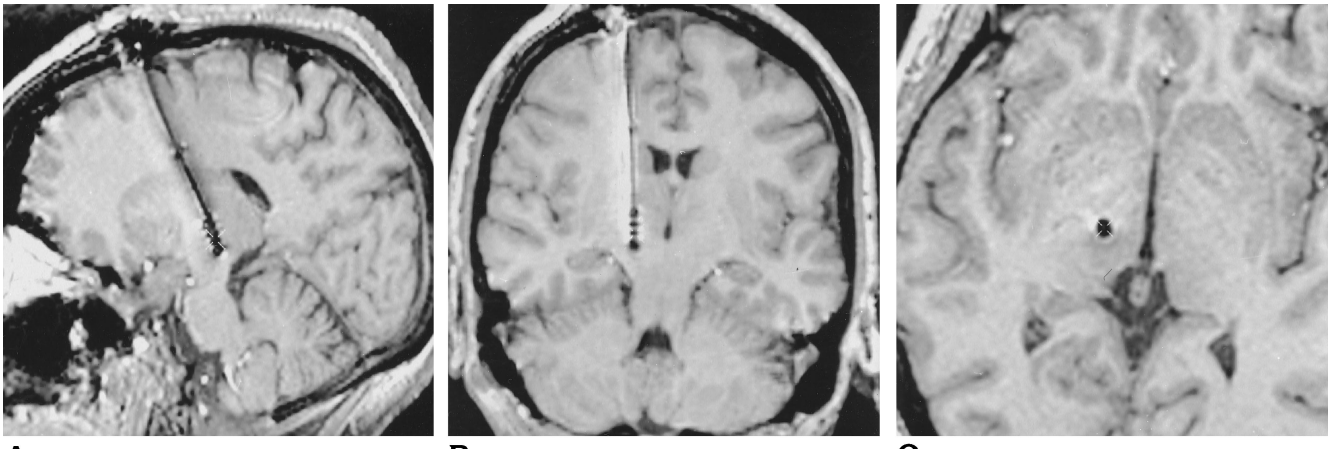

Fig 11. Same patient as in other figures. Control SPGR acquisitions (25/5/1, 25° flip angle) show the quadripolar electrode after implantation. The exact position of each contact can be ascertained by viewing it in three orthogonal planes. The 3-D cursor is in the same position in the sagittal (*A*), frontal (*B*), and axial (*C*) planes, and shows the actual contact used for the stimulation.

TABLE 2: Comparison of the chosen coordinates in the patient's reference system with the values determinated on the control examination

Patient	$(x'\ y')$Target	$(x'\ y')$Control	$(\lvert\Delta x'\rvert\ \lvert\Delta y\rvert')$
1	(−14.1 6.48)	(−13.7 5.9)	(0.38 0.58)
2	(−16.3 7.0)	(−16.8 7.5)	(0.45 0.49)
3	(−13 6.4)	(−12.8 6.6)	(0.2 0.16)
4	(−14.1 6.3)	(−12.4 8.9)	(1.7 2.6)
5	(−14.3 6.4)	(−13.2 6.3)	(1.1 0.18)

Note.—$(x'\ y')$target indicates chosen coordinates; $(x'\ y')$control, values of the coordinates on the control examination; $(\lvert\Delta x'\rvert\ \lvert\Delta y\rvert')$, absolute values of the errors for electrode position in the x' and y' directions; $\lvert\Delta x'\rvert$, $\lvert x'$ *target* − x' *control*$\rvert$, $\lvert\Delta y'\rvert$, $\lvert y'$ *target* − y′ *control*$\rvert$. All values are in millimeters.

trode. The four contacts of the 3387 quadripolar electrode were clearly identified on the 3-D SPGR acquisitions (Fig 11). Values of the chosen coordinates of the target and the coordinates determined on the control study (in the patient's reference system) are given in Table 2. Absolute values of the errors were less than one pixel for the first three cases, higher than one pixel in the x' and y' directions for case 4, and slightly higher than one pixel in the x' direction for case 5. The mean absolute value of the error in the x' direction for the electrode position (x' of the target − x' of the control) was 0.77 mm ± 0.6 (mean ± SD) and in the y' direction 0.80 mm ± 1.02. No iatrogenic lesions were detectable on the control studies; in particular, there were no hematomas or infarcts.

In all cases, the coordinates were calculated for the intersection of the electrode's trajectory with the AC-PC plane (z' = 0) in the patient's reference system. In an attempt to normalize the results among patients, these values were corrected by using the width of the third ventricle for the lateral (x') coordinate (ie, half the width of the third ventricle was subtracted from the lateral coordinate) and the length of the AC-PC line for the y' coordinate (ie, for each patient the y' coordinate was divided by the value of the AC-PC distance and multiplied by the mean of the AC-PC values in the five patients [26.2 mm]).

Table 3 gives the coordinates of the intersection of the electrode's trajectory normalized and nonnormalized in the patient's reference system. The mean value of the lateral coordinate (x') of the intersection of the electrode's trajectory with the AC-PC plane was −13.4 mm ± 2.2 (mean ± SD) before normalization and −10.5 mm ± 1.07 after normalization. The mean value of the anteroposterior coordinate (y') was 6.6 mm ± 1.38 before and 6.5 mm ± 1.54 after normalization.

Postoperative Long-Term Clinical Results

Table 1 gives the postoperative clinical results for the five patients. The percentage of tremor amelioration was determined by two neurologists on the basis of criteria in part 3 of the UPDRS (for the patients with Parkinson disease), CRST criteria (for the patient with essential tremor), and on a global assessment of the patient's improvement. After the electrode implantation, a microthalamotomy-like effect was observed in one patient (case 1), which persists

TABLE 3: True and normalized values of the coordinates of the definitive electrode in the AC-PC plane

	Patient 1	Patient 2	Patient 3	Patient 4	Patient 5
(x' y')intersection	(−13.7 8.0)	(−16.8 5.3)	(−10.8 6.6)	(−12.4 8.9)	(−13.2 6.3)
(x' y')normalized	(−11.2 5.8)	(−11.9 4.9)	(−9.3 6.6)	(−9.7 9.0)	(−10.4 6.2)

Note.—(x' y')intersection indicates the true value in the patient's reference system of the coordinates of the intersection of the definitive electrode with the AC-PC plane; (x' y')normalized indicates normalized values.

8 months after the implantation. In three patients, results were considered to be excellent: the stimulation produced a 90% reduction of the tremor in two patients (cases 2 and 3) and an 80% reduction in the other patient (case 4). In the last patient (case 5), stimulation produced a 70% diminution of the tremor, but the postoperative period was relatively short for the clinical evaluation. No side effects were noticed. The intensity and frequency of the electrode stimulation are given in Table 1.

Discussion

Originally, neurosurgical interventions for the treatment of tremor and related movement disorders were done with the use of ventriculography (2, 3, 14–19). For chronic stimulation of the Vim nucleus, the first step is to calculate the theoretical position of this structure, since its exact location cannot be determined precisely with ventriculography. It is thus necessary to perform an electrophysiological exploration to exactly locate the Vim nucleus. Investigators experienced in the application of chronic stimulation techniques advocate the use of five parallel microelectrodes to explore the ventrolateral thalamus (9, 10). The definitive electrode is positioned in the location where tremor is arrested using minimal current intensity and where the threshold for side effects is the highest. Recently, some authors have suggested that MR- or CT-derived targets could be used for stereotactic ventrolateral thalamotomy (8, 22–29, 38). The aim of our study was to validate the use of 3-D MR imaging to guide the implantation of intrathalamic electrodes in patients with medically refractory tremor.

Use of Stereotactic MR Imaging for Functional Stereotaxy

MR imaging with high-field MR units allows excellent visualization of the commissures, the thalamic organization, and individual anatomic variations while reducing imaging artifacts produced by the stereotactic frame (27). With 3-D gradient-echo acquisitions it is possible to obtain millimetric sections with good signal/noise ratio. High-field MR imaging enables the radiologist to noninvasively locate all the anatomic landmarks that are identified by ventriculography. In addition, structures not seen on ventriculograms, such as the internal capsule, can be visualized.

Concerns have been voiced that distortion on MR images might displace intracranial targets from their true anatomic location (39), leading to errors in determining target coordinates and, consequently, to unsuccessful stereotactic procedures. However, precise MR-guided stereotactic procedures can be performed using high-field MR imaging with a homogeneous magnetic field and linear field gradients (31, 32, 40). Using anatomic specimens, the mean stereotactic errors have been reported to be 0.48 ± 0.17 mm, 0.69 ± 0.14 mm, and 0.82 ± 0.13 mm in the x, y, and z directions, respectively (32). These results support the fact that functional MR imaging procedures can be performed safely after verifying the precision achieved with a specific stereotactic MR installation.

We used 3-D SPGR sequences to obtain thin sections (1.3 mm), acquired in the axial plane to minimize image distortion, as described by Derosier et al (31). Calculations of the stereotactic coordinates were made using the Advantage Windows workstation and the Voxtool software. This software allowed automatic identification of the fiducial markers of the frame. The small value (less than 1 mm) of the mean distance between the theoretical fiducial markers and the position of the fiducial markers on the 3-D SPGR acquisitions allowed us to confirm for each patient the absence of any significant image distortion. Registration of the acquisition in the stereotactic reference system allowed easy determination of the stereotactic coordinates of any anatomic landmark. It also

allowed correction of any rotation of the stereotactic frame in reference to the axis of the MR unit.

Determination of the Target and of the Electrode Trajectory

The principle for determining the target and the electrode trajectory was to use the same anatomic landmarks as those used with ventriculography (ie, AC, PC, width of the third ventricle, and height of the thalamus). The Guiot parallelogram (4) is a graphic method commonly used to locate the Vim nucleus (9, 10, 12). Usually, this parallelogram is drawn on the ventriculogram. Our method allows an analytic determination of the Guiot parallelogram that is more precise than the conventional graphic method. Moreover, the use of 3-D MR acquisitions and 3-D software makes it easy to determine the midline sagittal plane. The position of the head in the frame has no influence on the precision of the technique, as any rotation or lateral tilting can be easily corrected. The use of MR imaging permits accurate determination of the height of the thalamus and the width of the third ventricle at the level of the target's position. Frequently, the width of the third ventricle is not the same anteriorly as posteriorly and thus cannot be accurately calculated on a ventriculogram.

Modifications of the Trajectory

When ventriculography is used to determine the location of the Vim nucleus, most investigators do not perform angiography; consequently, no information is available about vascular structures. The use of MR angiography allows visualization of cortical vessels and subependymal veins.

With ventriculography, the chosen trajectory is in a parasagittal plane and, often, transventricular. Our 3-D method allows one to obtain an extraventricular trajectory with a double obliquity (anterior and lateral). This trajectory avoids subependymal veins; however, the final trajectories are only slightly different from the theoretical parasagittal trajectory. These modifications thus have no consequences for electrophysiological exploration.

Intraoperative Control Studies

When stereotactic MR imaging is used, the coordinates of the anatomic landmarks of the third ventricle and, consequently, those of the Vim nucleus are known in the stereotactic reference system. During the surgical procedure, use of anteroposterior and lateral X-ray films and X-ray fiducial markers makes it possible to control the stereotactic coordinates of the tip of the electrode.

The reason for these radiologic controls after stereotactic MR identification of the target is that exact positioning with millimetric precision of the definitive electrode is not straightforward using the needle-guiding device of the Leksell stereotactic frame. Moreover, the trajectory of an electrode could be deviated (eg, by the lateral ventricle). Special effort was made to position the definitive electrode in the same location as the exploring electrode that gave the best results.

The use of ventriculography for implantation of chronic stimulation electrodes (9–12) is thought to allow direct control of the position of the electrodes in relation to the anatomic landmarks of the third ventricle. These landmarks can be seen directly on the ventriculogram, allowing one to draw the position of the Vim nucleus by using the Guiot parallelogram. During the intervention, this position can then be graphically recorded on the radiologic control study showing the electrodes, since the position of the Vim nucleus in the stereotactic reference system is known. The control is thus indirect, because ventriculography is not performed during electrode positioning but hours beforehand.

Thus, with both ventriculography and stereotactic MR imaging, the coordinates of the Vim nucleus are known in reference to the stereotactic frame (in one case graphically and in the other analytically).

Results Obtained with Stereotactic MR Imaging for Functional Stereotaxy

The results of the intraoperative electrophysiological exploration show that in all our patients, stereotactic MR-determined trajectories were accurate and allowed us to find the position of the Vim nucleus. The postoperative MR results show that the electrodes were positioned correctly. Findings at clinical follow-up were excellent in all cases. The microthalamotomy-like

effect obtained in one patient suggests that a small lesion had been produced in the Vim nucleus during the electrophysiological study or during electrode implantation. This effect has already been described by Benabid et al (9), who reported a temporary suppression or reduction of the tremor after the surgical procedure that reappeared 1 to 10 days later, often at a lower amplitude than before surgery.

Postoperative Control Studies

The postoperative MR control studies allowed us to test the precision of our procedure by comparing the predefined target with the actual location of the electrode. These measurements assessed the precision of the entire procedure in terms of: MR determination of the target on the basis of the coordinates of AC, PC, and point K; display of the stereotactic coordinates on the frame; positioning of the final electrode; and MR determination of the coordinates of the electrode. Maximal theoretical precision of this procedure is limited by the finite size of the pixel. Imprecision in the determination of the coordinate of the target is plus or minus half the value of one pixel. The same imprecision should be observed when determining the coordinates of the final electrode. It is thus possible to obtain an imprecision of plus or minus one pixel for the entire procedure, even if the error in setting the coordinates and positioning the electrode is equal to zero. The value of one pixel is 0.94 mm, thus the imprecisions in the x' and y' directions for the first three cases can be explained by the finite size of the pixel. Greater imprecision in our case 5 can be explained by a small error in setting the coordinates and/or in positioning the final electrode (0.2 mm). It is only in case 4 that significantly greater imprecision was observed, suggesting an additional 0.8-mm error in the x' direction and a 1.7-mm error in the y' direction. The mean errors in the x' (0.77 mm) and the y' (0.8 mm) directions were, however, both less than one pixel, indicating good accuracy. The fact that these measurements indicate the precision of the entire procedure suggests that the precision of MR target determination is probably superior to the one determined by means of the postoperative MR control studies.

During exploration, the clinical and neurophysiological findings were dependent on the z coordinate. The data showed that the accuracy was good in the z direction because the maximum effect was always obtained at the level of the predetermined AC-PC plane. However, we made no attempt to quantify the precision of the z positioning of the stimulating electrode, because it is surgically impossible to obtain millimetric precision in the superoinferior direction. At the end of the procedure, the electrode is fixed manually to the skull, and there is a risk of minimal postoperative displacement in the z direction. On the other hand, in the x and y directions, the position is determined by the arch of the stereotactic frame with millimetric precision. This imprecision of the procedure in the z direction is of no consequence, because we used (like all investigators who perform thalamic stimulation) a four-contact electrode. Stimulation is provided by only one contact, which is chosen after the intervention. If necessary, this contact can be changed even months after the intervention.

An interesting feature of the postoperative control study was the comparison of the best target (as determined on the control study) among patients. The most striking result was the relatively low variability in the patients' coordinates. This was especially true for the y' coordinate, which had an SD of 1.38 mm. As for the x' coordinate, variability was greater before normalization (SD = 2.2 mm) than after (subtraction of half the width of the third ventricle; SD = 1.07 mm), suggesting that the major contributor to variability in the lateral coordinate is the width of the third ventricle, and that it is important to take into account this variation when calculating the theoretical target position. Conversely, normalization did not diminished the variability of the y' coordinate. This fact seems to be in opposition to the Talairach proportionality hypothesis; however, our patient series is too small to allow a definitive conclusion. We hope that further experience and evaluation of the results of postoperative MR control studies in larger series will help us improve the preoperative determination of the target.

Comparison with Ventriculography

The use of MR imaging under stereotactic conditions allows more simple and less invasive procedures because it avoids ventriculography. A comparison of the two techniques in terms of length of the procedure is difficult. The total duration of the stereotactic MR imaging proce-

dure is approximately 50 minutes, which is comparable to the time needed to perform ventriculography. Some authors (9), however, prefer to perform ventriculography with the patient under general anesthesia and not on the same day as electrode implantation. Thus, we have to compare an invasive procedure requiring general anesthesia with a more simple MR examination. Preoperative MR analysis with the Voxtool software and the Excel spreadsheet requires approximately 30 minutes, which is slightly longer than the time needed to draw the Guiot parallelogram on the ventriculogram. Operating room time is the same for both procedures. The duration of the stereotactic MR procedure was principally related to the neurophysiological study and to the implantation of the definitive electrode. During our study, this time decreased from 12 hours for the first patient to 5 hours for the last one. It could be significantly reduced by simplifying the electrophysiological exploration, which we think will be possible in the future.

To our knowledge, there are no published measurements of the precision of a ventriculography-guided stereotactic procedure. The precision that we obtained with stereotactic MR imaging (0.77 in the x direction and 0.8 in the y direction) is higher than the one needed for such a procedure. Benabid et al (9) reported obtaining tremor suppression with a low-intensity current at a distance of about 2 to 3 mm. As for stimulation thresholds, our data (mean threshold voltage = 2.1 V) are similar to those reported by Benabid et al (3.32 V for essential tremor and 2.97 V for Parkinson disease).

The reason to continue to use a method based on the AC-PC line is that the Vim nucleus is, at present, not directly visible by MR imaging. The MR signal is the same as the more posteriorly located ventroposterolateral nucleus and, thus, the boundary between these two nuclei is not apparent. Other targets of Parkinson disease, like the subthalamic nucleus (11) and the internal pallidum, are more clearly seen on MR images; thus, in the future, we think direct MR determination of the coordinates of these nuclei for electrode implantation will be feasible.

Conclusion

Our results show that MR imaging under stereotactic conditions is the procedure of choice for functional neurosurgery. As suggested by other authors, in the context of thalamotomy procedures (8), we consider that ventriculography is no longer necessary for implantation of stimulating electrodes. In addition, the use of MR angiography improves the safety of the procedure. Stereotactic MR imaging appears to be a promising technique for defining other targets in patients with Parkinson disease that are directly visible on MR images.

Acknowledgments

We thank Cécile Mazur, Christophe Messier, Marie Guibert, Sandrine Fellay, and Carole Vigie, the medical illustrators who executed the original drawings; M. Vidailhet, A. Benabid, and P. Pollak for helpful advice and discussions; and C. Derosier, who allowed us to use his stereotactic software.

Appendix

Calculation of the Coordinates of the Guiot Parallelogram in the Patient's Coordinate System

Using the geometric definitions of the Guiot parallelogram, we can derive the coordinates of the four corners, C2, C3, C4, and C5, on the patient's coordinate system as follows:

$$C2\begin{pmatrix}(-1)^n \times (11.5 + V/2)\\ D/6\\ 0\end{pmatrix}\ C3\begin{pmatrix}(-1)^n \times (11.5 + V/2)\\ D/4\\ 0\end{pmatrix}$$

$$C4\begin{pmatrix}(-1)^n \times (11.5 + V/2)\\ D/3\\ -h/2\end{pmatrix}\ C5\begin{pmatrix}(-1)^n \times (11.5 + V/2)\\ 5D/12\\ -h/2\end{pmatrix}$$

where n = 1 for the right thalamus and n = 2 for the left thalamus.

Calculation of the Transforming Coordinate Matrix

Our aim is to find the matrix that allows us to determine the stereotactic coordinates in the (O, **i, j, k**) system of a point, L, as a function of its coordinates in the patient's coordinate system (P, **i', j', k'**). We first calculate the matrix, M, as if the stereotactic reference system was centered on P, corresponding to a change from the system (P, **i', j', k'**) to (P, **i, j, k**). The stereotactic coordinates can then be obtained by a simple translation. The columns of M are given by the components of **i'**, **j'** and **k'** in the (**i, j, k**) system. In the (P, **i, j, k**) reference system (P is the center of PC), the coordinates of A (center of AC) are

$$\begin{pmatrix}x_a\\ y_a\\ z_a\end{pmatrix},$$

the coordinates of K (a point located in the midline sagittal plane)

$$\begin{pmatrix} x_k \\ y_k \\ z_k \end{pmatrix}.$$

The components of j' are

$$j' = \frac{\vec{PA}}{D} = \begin{pmatrix} \frac{x_a}{D} \\ \frac{y_a}{D} \\ \frac{z_a}{D} \end{pmatrix}$$

where D is the length of the AC-PC line.

The components of i' are

$$i' = \frac{\vec{PK} \wedge \vec{PA}}{\|\vec{PK} \wedge \vec{PA}\|} = \frac{1}{D_2}\begin{pmatrix} x_k \\ y_k \\ z_k \end{pmatrix} \wedge \begin{pmatrix} x_a \\ y_a \\ z_a \end{pmatrix} = \frac{1}{D_2}\begin{pmatrix} y_k z_a - z_k y_a \\ z_k x_a - x_k z_a \\ x_k y_a - y_k x_a \end{pmatrix}$$

with

$$D_2 = \|\vec{PK} \wedge \vec{PA}\| = \sqrt{(y_k z_a - z_k y_a)^2 + (z_k x_a - x_k z_a)^2 + (x_k y_a - y_k x_a)^2}$$

The components of k' are

$$k' = i' \wedge j' = \frac{1}{DD_2}\begin{pmatrix} x_a(z_a z_k + y_a y_k) - x_k(y_a^2 + z_a^2) \\ y_a(x_a x_k + z_a z_k) - y_k(z_a^2 + x_a^2) \\ z_a(y_a y_k + x_a x_k) - z_k(x_a^2 + y_a^2) \end{pmatrix}$$

The value of M is thus:

$$M = \begin{pmatrix} \frac{y_k z_a - z_k y_a}{D_2} & \frac{x_a}{D} & \frac{1}{DD_2}[x_a(z_a z_k + y_a y_k) - x_k(y_a^2 + z_a^2)] \\ \frac{z_k x_a - x_k z_a}{D_2} & \frac{y_a}{D} & \frac{1}{DD_2}[y_a(x_a x_k + z_a z_k) - y_k(z_a^2 + x_a^2)] \\ \frac{x_k y_a - y_k x_a}{D_2} & \frac{z_a}{D} & \frac{1}{DD_2}[z_a(y_a y_k + x_a x_k) - z_k(x_a^2 + y_a^2)] \end{pmatrix}$$

All these calculations have been integrated into the Excel (Microsoft) software which allowed us automatically to obtain the coordinates in the stereotactic coordinate system for any given point in the patient's coordinate system and vice versa.

References

1. Spiegel EA, Wycis HT, Marks M, Lee AJ. Stereotaxic apparatus for operations on the human brain. *Science* 1947;106:349–350
2. Talairach J, Paillas JE, David M. Dyskinésie de type hémiballique traitée par cortectomie frontale limitée, puis par coagulation de l'anse lenticulaire et de la portion interne du globus pallidus: amélioration importante depuis un an. *Rev Neurol* 1950;83:440–451
3. Hassler R, Reichert T. Indikationen und lokalisationen: Methode für gezeilten Hirnoperationen. *Nervenarzt* 1954;25:441–447
4. Guiot G, Arfel G, Derome P. La chirurgie stéréotaxique des tremblements de repos et d'attitude. *Gazette Medicale de France* 1968;75:4029–4056
5. Nagaseki Y, Shibazaki T, et al. Long-term follow-up results of selective VIM-thalamotomy. *J Neurosurg* 1986;65:296–302
6. Fox MW, Ahlskog JE, Kelly PJ. Stereotactic ventrolateralis thalamotomy for medically refractory tremor in post-levodopa era Parkinson's disease patients. *J Neurosurg* 1991;75:723–730
7. Jankovic J, Cardoso F, Grossman RG, Hamilton WJ. Outcome after stereotactic thalamotomy for parkinsonian, essential and other types of tremor. *Neurosurgery* 1995;37:680–687
8. Alterman RL, Kall BA, Cohen H, Kelly PJ. Stereotactic ventrolateral thalamotomy: is ventriculography necessary? *Neurosurgery* 1995;37:717–722
9. Benabid AL, Pollak P, Gervason C, et al. Long-term suppression of tremor by chronic stimulation of the ventral intermediate thalamic nucleus. *Lancet* 1991;337:403–406
10. Benabid AL, Pollak P, Seigneuret E, Hoffman DE, Gay E, Perret J. Chronic VIM stimulation in Parkinson's disease: essential tremor and extra-pyramidal dyskinesias. *Acta Neurochir Suppl (Wien)* 1993;58:39–44
11. Limousin P, Pollak P, Benazzouz A, et al. Effects on parkinsonian signs and symptoms of bilateral subthalamic nucleus stimulation. *Lancet* 1995;345:91–95
12. Blond S, Caparros-Lefebvre D, Parker F, et al. Control of tremor and involuntary movement disorders by chronic stereotactic stimulation of the ventral intermediate thalamic nucleus. *J Neurosurg* 1992;77:62–68
13. Caparros-Lefebvre D, Blond S, Vermersch P, Pécheux N, Guieu JD, Petit H. Chronic thalamic stimulation improves tremor and levodopa induced dyskinesias in Parkinson's disease. *J Neurol Neurosurg Psychiatry* 1993;56:268–273
14. Mohadjer M, Goerke H, Milios E, Etou A, Mundinger F. Long term results of stereotaxy in the treatment of essential tremor. *Stereotact Funct Neurosurg* 1990;54–55:125–129
15. Siegfried J. Therapeutic stereotactic procedures on the thalamus for motor movement disorders. *Acta Neurochir (Wien)* 1993;124:14–18
16. Krauss JK, Mohadjer M, Nobbe F, Mundinger F. The treatment of posttraumatic tremor by stereotactic surgery: symptomatic and functional outcome in a series of 35 patients. *J Neurosurg* 1994;80:810–819
17. Kelly PJ, Derome P, Guiot G. Thalamic spatial variability and the surgical results of lesions placed with neurophysiologic control. *Surg Neurol* 1978;9:307–315
18. Kelly PJ, Gillangham FJ. The long-term results of stereotaxic surgery and L-dopa therapy in patients with Parkinson's disease: a 10-year follow-up study. *J Neurosurg* 1980;53:332–337
19. Kelly PJ. Contemporary stereotactic ventralis lateral thalamotomy in the treatment of parkinsonian tremor and other movement disorders. In: Heilbrun MP, ed. *Stereotactic Neurosurgery*. Baltimore, Md: Williams & Wilkins; 1988:133–148
20. Hariz MI, Bergenheim AT, Fodstad H. Air-ventriculography provokes an anterior displacement of the third ventricle during functional stereotactic procedures. *Acta Neurochir (Wien)* 1993;123:147–152
21. Hariz MI, Bergenheim AT. A comparative study on ventriculographic and computerized tomography-guided determinations of brain targets in functional stereotaxis. *J Neurosurg* 1990;73:565–571
22. Hariz MI. Correlation between clinical outcome and size and site of the lesion in computed tomography guided thalamotomy and pallidotomy. *Stereotact Funct Neurosurg* 1990;54–55:172–185
23. Bucholz RD, Ho HW, Rubin JP. Variables affecting the accuracy of stereotactic localization using computerized tomography. *J Neurosurg* 1993;79:667–673
24. Laitinen LV. Brain targets in surgery for Parkinson's disease: re-

sults of a survey of neurosurgeons. *J Neurosurg* 1985;62:349–351
25. Laitinen LV. CT-guided ablative stereotaxis without ventriculography. *Appl Neurophysiol* 1985;48:18–21
26. Uematsu S, Rosenbaum AE, DeLong MR, et al. Magnetic resonance planned thalamotomy followed by X-ray/CT-guided thalamotomy. *Acta Neurochir Suppl (Wien)* 1987;39:21–24
27. Lunsford LD, Martinez AJ, Latchaw RE. Stereotactic surgery with a magnetic resonance and computerized tomography compatible system. *J Neurosurg* 1986;64:872–878
28. Rosenfeld JV, Barnett GH, Palmer J. Computed tomography guided stereotactic thalamotomy using the Brown-Roberts-Wells system for non-parkinsonian movement disorders: technical note. *Stereotact Funct Neurosurg* 1991;56:184–192
29. Whittle IR, O Sullivan MG, Ironside JW, Sellar R. Accuracy of ventrolateral thalamic nucleus localization using unreformatted CT scans and the B-R-W system: experimental studies and clinical findings during functional neurosurgery. *Acta Neurochir Suppl (Wien)* 1993;58:61–64
30. Kall BA, Goerss SJ, Kelly PJ. A new multimodality correlative imaging technique for VOP/VIM(VL) thalamotomy procedures. *Stereotact Funct Neurosurg* 1992;58:45–51
31. Derosier C, Delegue G, Munier T, Pharaboz C, Cosnard G. IRM: distortion géométrique de l'image et stéréotaxie. *J Radiol* 1991; 72:349–353
32. Dormont D, Zerah M, Cornu Ph, et al. A technique of measuring the precision of a MR-guided stereotaxic installation using anatomical specimens. *AJNR Am J Neuroradiol* 1994;15:365–371
33. Fahn S, Elton RL. UPDRS development committee: unified Parkinson's disease rating scale. In: Fahn S, Marsden CD, Calne DB, Goldstein M, eds. *Recent Developments in Parkinson's Disease.* New York, NY: Macmillan; 1987:2:153–163
34. Fahn S, Tolosa E, Marin C. Clinical rating scale for tremor. In: Jankovic J, Tolosa E, eds. *Parkinson's Disease and Movement Disorders.* Baltimore, Md: Urban and Schwarzenberg; 1988:225–234
35. Esteguy M, Bonnet AM, Kefalos J, Lhermitte F, Agid Y. Le test à la L-Dopa dans la maladie de Parkinson. *Rev Neurol* 1985;141: 413–415
36. Brooks ML, O'Connor MJ, Sperling MR, Mayer DP. Magnetic resonance imaging in localization of EEG depth electrodes for seizure monitoring. *Epilepsia* 1992;33:888–891
37. Zhang J, Wilson CL, Levesque MF, Behnke EJ, Lufkin RB. Temperature changes in nickel-chromium intracranial depth electrodes during MR scanning. *AJNR Am J Neuroradiol* 1993;14: 497–500
38. Hadley MN, Shetter AG, Amos MR. Use of the Brown-Roberts-Wells stereotactic frame for functional neurosurgery. *Appl Neurophysiol* 1985;48:61–68
39. Hassenbuch SJ, Pillay PK, Barnett GH. Radiofrequency cingulotomy for intractable cancer pain using stereotaxis guided by magnetic resonance imaging. *Neurosurgery* 1990;27:220–223
40. Kondziolka DE, Dempsey PF, Lunsford D, et al. Comparison between magnetic resonance imaging and computed tomography for stereotactic coordinate determination. *Neurosurgery* 1992;30: 402–407